Desalination and Water Treatment
www.deswater.com

doi: 10.5004/dwt.2019.24742

169 (2019) 322–332
November

Removal of Cd(II) from aqueous solution by sulfur-functionalized walnut shell: adsorption performance and micro-structural morphology

Xiuguo Lu, Jinjin Wu*, Yiting Guo

School of Civil Engineering and Architecture, East China Jiao Tong University, 808 East Shuanggang Road, Nanchang, 330013, China, Tel. +86 18255352574; email: 18255352574@163.com (J.J. Wu)

Received 26 March 2019; Accepted 22 July 2019

ABSTRACT

The sulfur-containing functional group was grafted onto walnut shell with xanthate to synthesize a biosorbent (SWM) for removal of cadmium in water. The synthesized adsorbent was characterized by scanning electron microscopy, Brunauer–Emmett–Teller (BET), Fourier transform infrared spectroscopy and X-ray photoelectron spectroscopy. And the mechanism was further analyzed by pH_{PZC} determination. The effects of pH, dosage, contact time, Cd(II) concentration and temperature on adsorption were investigated. Moreover, adsorption kinetics, adsorption isotherms and adsorption thermodynamics were studied. The results showed that the adsorption performance of SWM was better than unmodified walnut shell due to ion exchange and high-density sulfur-containing functional group on surface. The Cd(II) adsorption on SWM was found to follow Langmuir isotherm model with maximum adsorption capacity of 17.79 mg g^{-1}. And the adsorption was well described by pseudo-second-order kinetic model, the adsorption process was completed by three sections and the intraparticle diffusion process was not the only control step. Furthermore, the adsorption process was spontaneous and exothermic. All the results showed that the high adsorption performance of SWM make it a potential biosorbent in the treatment of cadmium contaminated water.

Keywords: Walnut shell; Xanthate; Cadmium; Adsorption

1. Introduction

Metal cadmium is a non-essential element for human body. Cadmium existing under natural conditions usually has little impact on organisms and the environment, while cadmium pollution caused by human activities such as mining, smelting, transportation and metal processing is potentially toxic to organism [1–4], and has relative mobility in the water-soil-plant system [5]. When cadmium is absorbed by human body through the food chain and respiratory system, it can cause heart disease, kidney failure, bone decalcification and other dysfunction diseases [6], the Minamata disease that occurs in Japan is caused by eating cadmium-containing rice. And the presence of cadmium in plants can cause adverse symptoms such as growth retardation, changes in photosynthesis, and interference with mineral absorption. Therefore, removal of cadmium is one of the key targets of water purification.

Currently, several methods have been applied to the removal of heavy metals in aqueous solutions, such as ion exchange, filtration, membrane separation, chemical precipitation, solvent extraction, electrochemical precipitation and adsorption [7–11]. Chemical precipitation requires a long processing time and prone to form insoluble compounds, which requires subsequent processing [12]. For ion exchange, conventional ion exchange resins cannot selectively adsorb ions in contaminated water [13]. Special modification of ion exchange resins can effectively remove heavy metals from

* Corresponding author.

contaminated water, but the cost is high and difficult for wide application. Thus, compared with other methods, adsorption has received more and more attention due to its advantages such as simplicity of operation, low cost and strong regenerative capacity.

Natural materials or agricultural wastes, such as sunflower [14], bagasse [15], coconut shell [16], orange peel [17], are available in large quantities and environmentally friendly, have some characteristics such as high carbon content and low ash content [18], often used as a precursor for the preparation of adsorbents. As a kind of agricultural and forestry waste, walnut shell is rich in lignin, cellulose and hemicellulose, and it contains many functional groups which have a strong affinity for heavy metal ions [19]. China's walnut planting area ranks first in the world, so the output of walnut shell is very considerable, which makes the walnut shell cheap and easy to obtain. At the same time, due to the high hardness, the walnut shell cannot be used for biological feed and other purposes, so how to properly apply a large amount of walnut shell waste is particularly important [20]. Some scholars have proved that the walnut shell–derived adsorbents have an adsorption effect on heavy metal in aqueous solution. Yang et al. [19] loaded a nanoscale zero-valent iron on a walnut shell to obtain a new composite material for removing Cu(II) and Ni(II) in water. The results showed that the maximum adsorption capacity for Cu(II) and Ni(II) was 458.7 and 327.9 mg/g, respectively. Ding et al .[21] incorporated nickel hexacyanoferrate into walnut shell to effectively deal with cesium in aqueous solution while also overcoming the difficulty of separating nickel hexacyanoferrate nanoparticles from solution. Xie et al. [22] found that the acid-modified walnut shell exhibited excellent adsorption performance for Cu(II) with a maximum adsorption capacity of 204.08 mg/g.

In fact, the walnut shell without any treatment has a poor adsorption effect on heavy metals, so it needs to be modified to improve its adsorption performance. However, the modification methods are still relatively simple, mainly acid modification, alkali modification and salt modification. Segovia-Sandoval et al. [23] modified the walnut shell with citric acid and studied its application in the removal of Zn(II). Zhu et al. [24] modified walnut shells with fatty acid studied its function in removing naphthalene. Chomiak et al. [25] used KOH to activate walnut shell-based carbon to prepare a series of microporous granular activated carbon. In general, modification methods need to be diversified. According to the hard and soft acids and bases theory [26], the sulfur-containing functional group is a soft ligand group, which has strong affinity for most heavy metal ions belonging to Lewis soft acid, and the functional group can be used to enhance the heavy metal removal capacity by complexation. The absolute hardness parameter of Cd(II) is 10.3, so the sulfur-containing functional groups are prone to forming stable complex with it. Further, the process of xanthate functionalization is simple, and the complex formed is stable. Therefore, it is feasible to use xanthate to graft the sulfur-containing functional group onto the walnut shell.

The main purpose of this work is to synthesize a low-cost biosorbent which contains the sulfur-containing functional group for efficient removal of cadmium from aqueous solution. Then, the adsorption performance of Cd(II) was studied, and the adsorption process was evaluated through the adsorption thermodynamics, adsorption kinetics and adsorption isotherm models. These results would provide a reliable basis for further application of low cost and high removal efficiency adsorbent prepared form walnut shell in actual contaminated water treatment.

2. Materials and methods

2.1. Materials

The walnut shell was purchased from Gongyi Water Purification Material Factory (Zhengzhou, Henan). The cadmium stock solution was prepared by dissolving high-purity cadmium powder in a small amount of 1:1 (V/V) nitric acid and freshly diluted with 1% hydrochloric acid to predetermined cadmium solution. All of the chemicals used in this study were analytical grade.

2.2. Modified biochar preparation

Modified biochar was prepared as follows according to the literature [27]. Typically, the walnut shell with a particle size of 0.4–0.8 mm was washed with deionized water to remove surface impurities, and dried at 80°C, obtained the original walnut shell, which was recorded as OW. Then, the walnut shell (OW) was soaked in concentrated sulfuric acid to obtain carbonized walnut shell (CW). Next, the CW was mixed with NaOH and CS_2 for xanthogenization (SW). Finally, the SW was modified with $MgSO_4$ (SWM), by which magnesium ion could be introduced to the biochar to increase the stability of the adsorbent.

Specific preparation steps are shown in Fig. 1.

$$\underset{\textbf{CW}}{(C_6H_9O_4OH)_n} + n\text{NaOH} \xrightarrow[25\,℃,\,90\text{min}]{1:3} (C_6H_9O_4ONa)_n + nH_2O \quad (1)$$

$$(C_6H_9O_4ONa)_n + nCS_2 \xrightarrow[25\,℃,\,60\text{min}]{1:1} \underset{\textbf{SW}}{nC_6H_9O_4OC{=}SSNa} \quad (2)$$

$$\underset{\textbf{SW}}{2C_6H_9O_4OC{=}SSNa} + MgSO_4 \xrightarrow[20\text{min}]{25℃} \underset{\textbf{SWM}}{C_6H_9O_4OC{=}SSMgSS{=}COO_4H_9C_6} + Na_2SO_4 \quad (3)$$

Fig. 1. The systemic procedure of the sulfar-functionalized walnut shell.

2.3. Modified biochar characterization

All the prepared modified biochar samples were analyzed before and after modification. The examined characteristics were (i) surface structure and composition, observed by Sigma HD thermal field emission scanning electron microscopy (SEM; Zeiss, Germany); (ii) pore volume and specific surface area, determined by ASAP2020 fast specific surface and porosity analyzer (Micromeritics, USA), using N_2 adsorption–desorption experiment at low temperature; (iii) surface functional groups, scanned by Nicolet iS10 Fourier infrared spectrometer (Thermo Fisher Scientific, United States) to obtain the infrared spectrum at a range of 400–4,000 cm^{-1}; (iv) surface energy, performed by X-ray photoelectron spectroscopy (K-Alpha$^+$, Thermo Fisher Scientific, USA) with Al Kα radiation; (vi) pH_{PZC}, 100 mL of 1.0 M KCl solution was added in an Erlenmeyer flask, the pH of the KCl solution was adjusted to 2–11 with 0.01 M HCl or 0.01 M NaOH, respectively. 0.1 g of OW or SWM were added to the solution, and stirred (200 rpm) at room temperature (25°C) for 24 h. Then, the supernatant was taken to determine the pH of the solution after centrifugation (4,000 r/min), that is, the equilibrium pH. The pH_{pzc} value can be obtained by plotting the initial pH as the abscissa and the equilibrium pH as the ordinate.

2.4. Batch experiments

The experiments were carried out by mixing a given amount of adsorbent with 50 mL of a cadmium solution. The pH of the solution was adjusted with 0.1 M NaOH or 0.1 M HNO_3. And the mixture was stirred (180 rpm) for a certain time using a constant-temperature vibrator. Finally, the supernatant was taken to analyze the change of cadmium concentration by 280FS AA fast sequential flame atomic absorption spectrometer (Agilent, Australia).

The effect of initial pH on adsorption was evaluated at pH in the range of 3.0–8.0. The effect of adsorbent dosage on adsorption was evaluated by changing the dosage from 1.0 to 25 g/L. For adsorption kinetics studies, the mixture was stirred for 5–2,880 min. The adsorption isotherm experiments were investigated with different cadmium concentration of 50, 80, 100, 120, 150, 180, 200 and 250 mg/L, respectively. For adsorption thermodynamics, the experiment was carried out at different temperatures, that is, 25°C, 30°C, 35°C, 45°C and 55°C.

2.5. Data analysis methods

The amount of Cd(II) adsorbed on adsorbents was calculated from Eqs. (4) and (5):

$$R = \left[\frac{\left(C_0 - C_e\right)}{C_0}\right] \times 100\% \tag{4}$$

$$q_e = \frac{\left[\left(C_0 - C_e\right) \times V\right]}{m} \tag{5}$$

where R (%) is the removal rate, C_0 (mg/L) and C_e (mg/L) are the initial and equilibrium concentration of Cd(II), respectively, q_e (mg/g) is the equilibrium adsorption capacity, V (L) is the volume of the Cd(II) solution, and m (g) is the weight of adsorbent used in the experiments.

The experimental data were fitted by the pseudo-first-order kinetic model, the pseudo-second-order kinetic model and the intraparticle diffusion model. These models can be expressed as Eqs. (6)–(8):

$$\ln\left(q_e - q_t\right) = \ln q_e - K_1 t \tag{6}$$

$$\frac{t}{q_t} = \frac{1}{K_2 q_e^2} + \frac{t}{q_e} \tag{7}$$

$$q_t = K_{\mathrm{id}}^{0.5} + C_{\mathrm{id}} \tag{8}$$

where q_t (mg/g) is adsorption capacity at time t, K_1 (1/min) is the rate constant of the pseudo-first-order model, K_2 (g/(mg min)) is the rate constant of the pseudo-second-order model, K_{id} (mg/g $min^{-0.5}$) is the intraparticle diffusion rate constant, C_{id} (mg/g) is the degree of boundary layer effect.

The experimental data were fitted by the Langmuir isotherm, the Freundlich isotherm and the Temkin isotherm. These isotherms can be expressed as Eqs. (9)–(11):

$$q_e = \frac{q_m K_L C_e}{\left(1 + K_L C_e\right)} \tag{9}$$

$$q_e = K_F C_e^{1/n} \tag{10}$$

$$q_e = \left(\frac{R_T}{b_T}\right) \ln a_T + \left(\frac{R_T}{b_T}\right) \tag{11}$$

For the Langmuir isotherm, its basic characteristic can be described by the separation factor R_L. It can be calculated using Eq. (12):

$$R_L = \frac{1}{\left(1 + K_L C_0\right)} \tag{12}$$

where q_m (mg/g) is the saturated adsorption capacity, K_L (L/g) is Langmuir constant, which is related to the adsorption intensity, K_F (μg/g) and n are Freundlich constants, which are related to the adsorption intensity and adsorption capacity, respectively, a_T (L/mg) is the equilibrium binding constant, which is related to the maximum binding energy, b_T (kJ/mol) is Temkin constant, which is related to the adsorption heat, R is the universal gas constant, it is defined by 8.314 J mol^{-1} K^{-1}, and T (K) is the absolute temperature.

The relevant thermodynamic parameters of adsorption can be obtained from Eqs. (13) to (15):

$$\ln K = -\left(\frac{\Delta H}{RT}\right) + \left(\frac{\Delta S}{R}\right) \tag{13}$$

$$\Delta G = -RT \ln K \tag{14}$$

$$K = \frac{q_e}{C_e} \tag{15}$$

where K is the partition coefficients at each temperature, ΔH (kJ/mol) is the enthalpy change, ΔS (kJ/mol) is the entropy change and ΔG (kJ/mol) is the Gibbs free energy change.

3. Results and discussion

3.1. Characterization of adsorbent

3.1.1. SEM observation

The morphologies and microstructures of OW and SWM were observed by SEM at different magnifications. As can be seen from Fig. 2, OW showed a sheet-like morphology and smooth surface. Only a small amount of pores appeared on surface and the arrangement is randomly uneven. However, the structure of SWM changed greatly. It revealed a honeycomb morphology and the surface was more wrinkled and more rough. The pore structure was developed, a large number of pores were uniformly and orderly arranged on the surface. The development of pore structure and roughness of the surface should be considered as factors that increase the surface area of material [28], which would improve the adsorption performance of material. Overall, the modification treatment successfully changed the morphologies and microstructures of the material.

3.1.2. BET analysis

Within the limited volume of adsorbent, the larger specific surface area allows for more pores on surface [29]. Therefore, the specific surface area has a major influence on the adsorption. At the same time, the pore volume was also an important factor determining the adsorption performance of the adsorbent. It can be seen from Table 1 that the pore volume of SWM is 0.164 cm^2/g, which is 2.16 times that of OW. The specific surface area of SWM is 214.39 m^2/g, which is 4.98 times that of OW. It can be seen that the modification treatment can improve the pores of the walnut shell. The specific surface area can provide more adsorption sites for adsorption and improve the adsorption capacity of the material.

3.1.3. Fourier transform infrared spectroscopy analysis

Fourier transform infrared spectroscopy (FT-IR) was characterized to confirm possible chemical bonds of synthetic products in the range of 4,000~400 cm^{-1}. As is shown in Fig. 3, for OW, a broad peak at 3,448 cm^{-1} was assigned to the stretching vibration of O–H functional groups [30]. The band at 1,635 cm^{-1} denoted the C=O stretching vibration of aromatic, and the band at 1,041 cm^{-1} denoted the superposed vibration absorption peak of C–O. These bands above were the adsorption bands that all plant-based materials contain [31]. In addition, the bands at 2,922 cm^{-1} was assigned to the C–H stretching vibrations of CH_2 groups [29], the bands at 1,509 cm^{-1} denoted the in-plane vibration of C=C due to the aromatic ring vibration of lignin in walnut shell [32]. The bands at 1,380 cm^{-1} was assigned to the stretching vibration of the $-CH_3^-$ in cellulose and hemicellulose [33]. However, as for SWM, it showed stretching vibration of O–H and the in-plane vibration of C=C originally present in OW disappeared, and the deformation vibration of $-CH_3^-$ at 1,378 cm^{-1} was more pronounced. This is due to the fact that xanthate can reduce the lignin and hemicellulose contained in the walnut shell, and the cellulose content was relatively increased to form cellulose xanthate [31,33,34], Besides, many new adsorption bands appeared in SWM.

Table 1
BET analysis of OW and SWM

Sample	Pore volume (cm^2/g)	Specific surface area (m^2/g)
OW	0.076	43.03
SWM	0.164	214.39

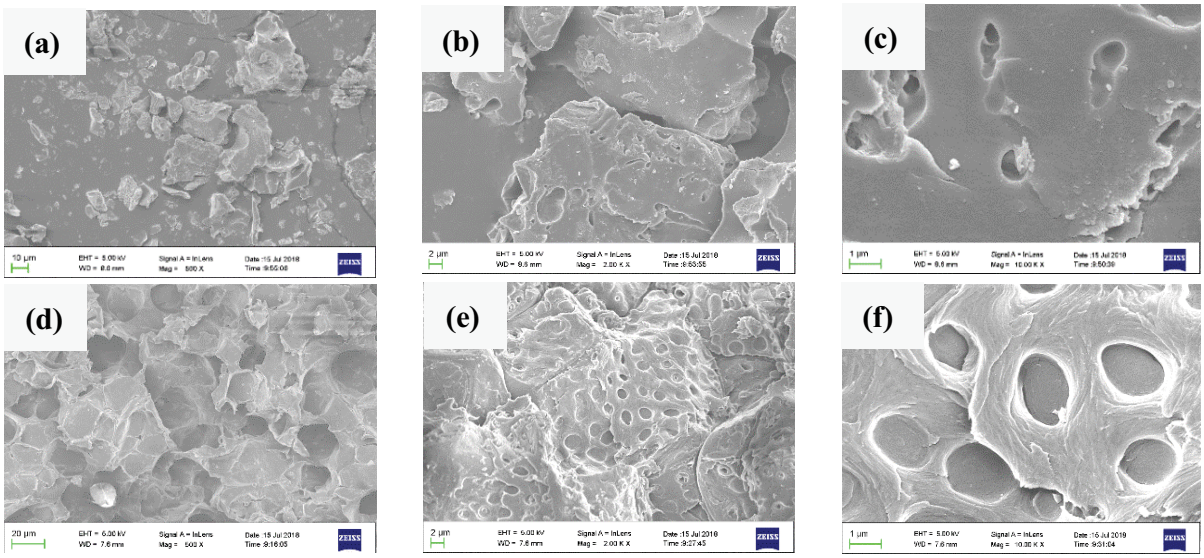

Fig. 2. SEM image of OW (a, b, c) and SWM (d, e, f).

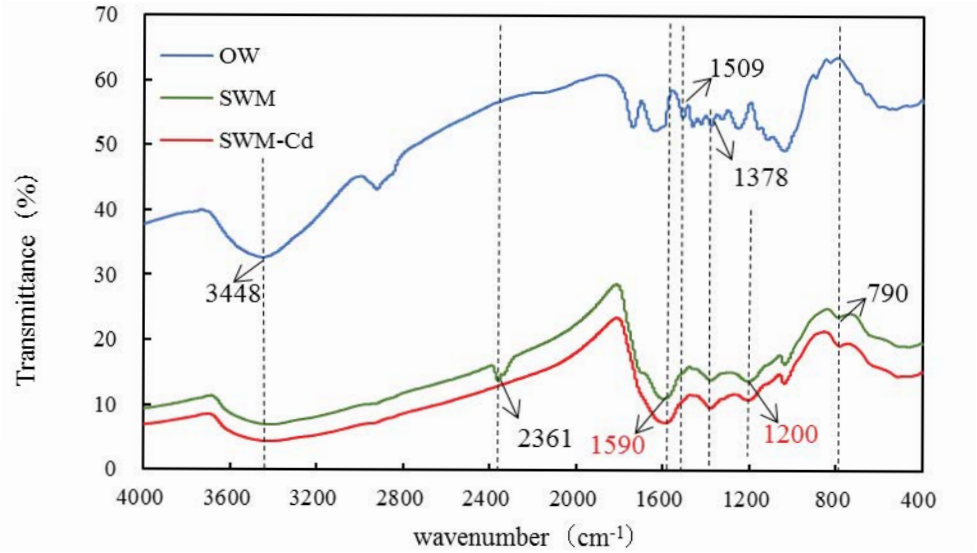

Fig. 3. FT-IR spectra of OW, SWM and SWM-cd.

The bands at 2,361 cm^{-1} denoted the stretching vibration of –SH. The band at 1,590 cm^{-1} was the anti-symmetric stretching vibration of –COO–. The bands at 1,200 cm^{-1} indicated the stretching vibration of –C=S. The band at 790 cm^{-1} was the stretching vibration of –C–S. Among them, the –COO– adsorption band was more obvious, because the concentrated sulfuric acid with strong oxidizing property was used for carbonization and dehydration in the preparation process of SWM, so that the C atom in the reduced state was oxidized to form –COO–. Moreover, the appearance of –C=S and –C–S adsorption bands indicated that the xanthation modification was successfully carried out, and the xanthate group was successfully grafted onto the OW. After adsorption, the adsorption bands such as –C=S, –C–S and $–COO^-$ became weaker and broader. It was speculated that the S in the –C=S and –C–S group formed a coordinate bond with the heavy metal Cd, thereby causing a change in the corresponding absorption band of the group. Furthermore, the absorption band of –SH disappeared, indicating that the sulfhydryl group participated in the adsorption reaction and it was an effective adsorption group.

3.1.4. X-ray photoelectron spectroscopy (XPS) analysis

XPS was used to analyze the modification process of OW to SWM and Cd(II) adsorption process on SWM. As can be seen from Fig. 4a, the XPS survey scan of OW only showed C 1s, N 1s and O 1s peaks at 284.08, 401.08 and 534.08 eV, respectively. After modification, the main characteristic peaks of SWM consist of S 2p (168.08 eV), C 1s (285.08 eV), N 1s (401.08 eV), O 1s (532.08 eV), Na 1s (1,071.08 eV). And the peak of Cd 3d (405.62 eV) appeared after adsorption, indicating that the heavy metal Cd was successfully adsorbed on SWM. The characteristic peaks of S $2p_{1/2}$ and S $2p_{3/2}$ of each sulfur component before and after adsorption were observed as shown in Figs. 4b and c. There were three types of sulfur before adsorption including SO_4^{2-} (169.38eV) introduced from the treatment of concentrated sulfuric acid, C=S (168.18 eV) and –SH (164.08 eV) attributed to the treatment of CS_2 [35]. However, as can be seen from Fig. 4c, peak at 168.08 showed little change compared with peak of SWM before adsorption, and peak of –SH disappeared after adsorption, which was consistent with the results obtained in FT-IR spectra, suggesting that C=S play a small role in adsorption process and –SH participated in the adsorption of Cd(II) and formed a complex with it. Moreover, the magnesium content before and after adsorption was compared, and it was found that the content of magnesium decreased after adsorption (0.25–0.13). It is speculated that ion exchange may have taken place during the adsorption process, which was the reason for the lower magnesium content. As shown in Fig. 4d, the binding energies of Cd $3d_{3/2}$ and Cd $3d_{5/2}$ for SWM after adsorption were 412.28 and 405.58 eV, respectively. This indicated that a metal cadmium ion reacted with two thiol groups to form a bidentate complex, similar with lead sulfide clusters, which was the same result as a bidentate complex formed by a sulfhydryl-based activated carbon adsorbent and a metal ion [36].

3.1.5. Determination of pH_{pzc}

The zero point of charge (pH_{pzc}) refers to the pH value when the positive and negative charges on the surface of the adsorbent are equal. For the same adsorbent, its pH_{pzc} value is certain, but when the pH of the solution is different, the surface electronegativity and surface charge of the adsorbent are different. Fig. 5 shows the pH_{pzc} curve of OW and SWM. As can be seen from the figure, the pH_{pzc} value of OW and SWM was 6.03 and 7.18, respectively. It indicated that the pH_{pzc} value increased from 6.03 to 7.18 due to xanthation, which means the modified adsorbent pH_{pzc} is closer to neutral. In addition, Fig. 5 also reflects the strong pH buffering capacity of SWM. Although the initial pH value of the solution changes greatly (2–11), it can finally maintain the pH value of the solution system at around 7.1. When $pH < pH_{pzc}$, the surface of the adsorbent is positively charged.

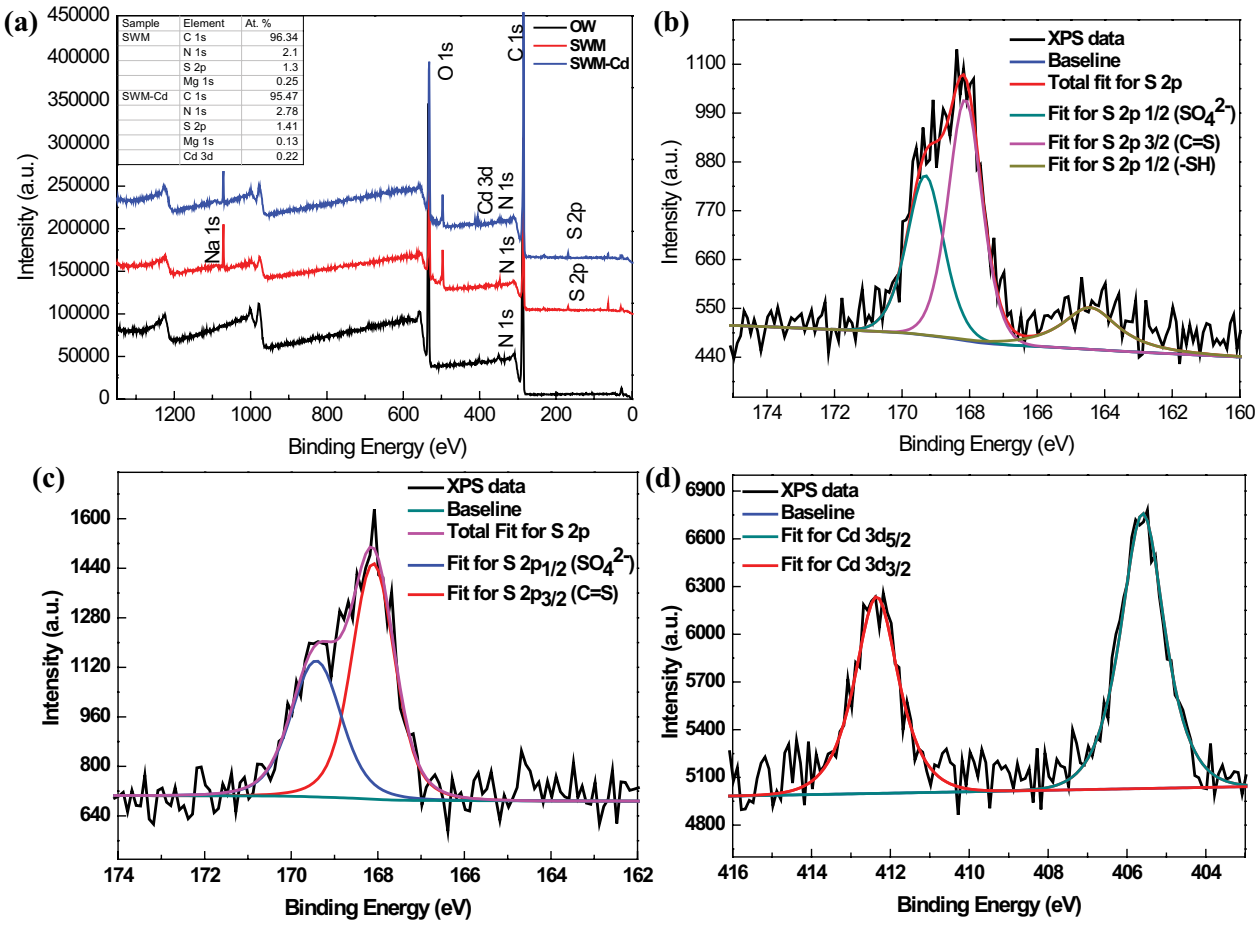

Fig. 4. (a) XPS survey scan spectra of OW, SWM and SWM-Cd; (b) XPS high resolution spectra of S 2p for SWM; (c) XPS high resolution spectra of S 2p for SWM-Cd; (d) XPS high resolution spectra of Cd 3d for SWM-Cd.

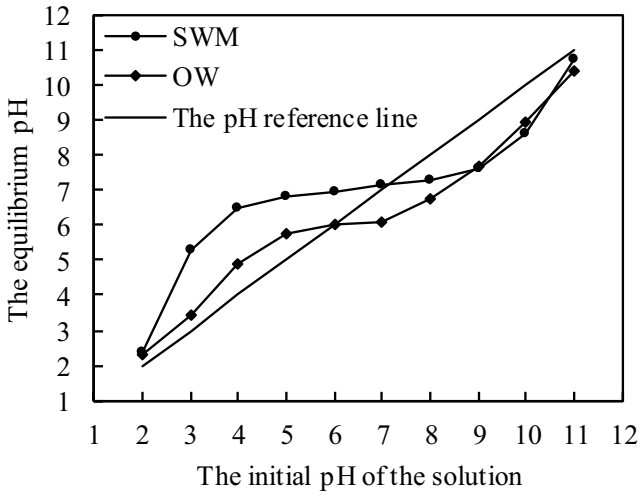

Fig. 5. Relationship between the initial pH and the equilibrium pH.

When pH = pH_{pzc}, the surface of the adsorbent is electrically neutral. When pH > pH_{pzc}, the surface of the adsorbent is negatively charged [37]. The larger the negative charge on the surface of the adsorbent, the better the adsorption effect, which means that the adsorption properties of OW and SWM will be improved when the pH is higher than 6.03 and 7.18, respectively.

3.2. Adsorption of Cd(II)

3.2.1. Effect of initial pH

The initial pH of the solution plays an important role in adsorption process owing to its influence on metal ion forms in the solution, surface charge of adsorbents and the competitiveness of H^+ [28,38]. The effect of initial pH of the solution on adsorption is shown in Fig. 6. It can be observed that the initial pH dramatically influenced the Cd(II) removal of adsorbent. When the pH value was lower than 7.0, the Cd(II) removal rate of OW increased with the increase of pH value. When the pH was 7.0, the removal rate of OW reached highest at 45%. When pH was higher than 7.0, the removal rate of OW was decreased. This was because when the pH was low, the degree of protonation was higher, which led to the positive charge density increase of OW and stronger electrostatic repulsion. At the same time, Cd(II) suffered competitive adsorption with H^+ and H_3O^+, so the removal rate increased with the increase of initial pH. Besides, Cd(II) precipitated in the form of $Cd(OH)_2$

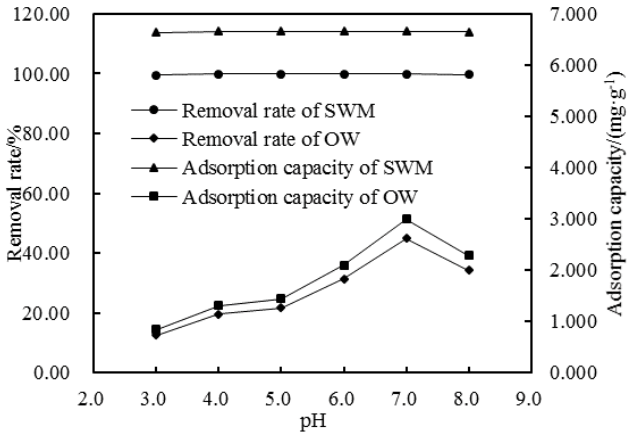

Fig. 6. Effect of initial pH on Cd(II) adsorption.

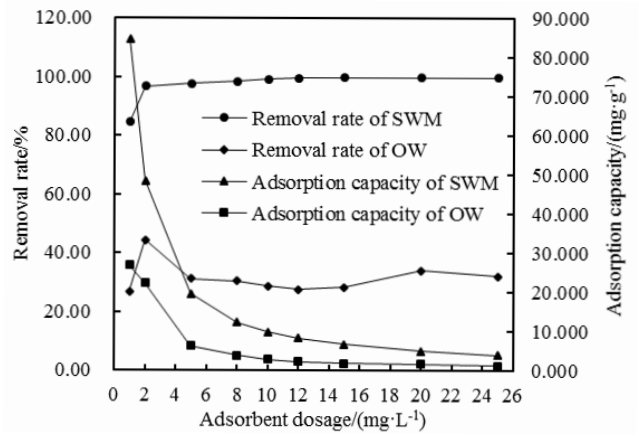

Fig. 7. Effect of adsorbent dosage on Cd(II) adsorption.

and $Cd(OH)_3^-$ when the pH was above 7.0, so the amount of free ions decreased, which affected the adsorption effect. As for SWM, a maximum removal rate of 99.90% was obtained at pH 7.0. However, regardless of the pH value, the Cd(II) removal rate of SWM was all above 99%, indicating that the modified walnut shell has a wide range of application to the pH of the solution and high removal efficiency of Cd(II). The experiment results were coincident with the analysis of pH_{pzc}, in consideration of the pH_{pzc} value, the optimum pH of SWM was determined to be 7.0 for further study.

3.2.2. Effect of adsorbent dosage

The effect of adsorbent dosage on Cd(II) removal was studied and the results are shown in Fig. 7. With the increase of adsorbent dosage, the Cd(II) removal rate of OW and SWM increased, the adsorption capacity decreased. Further, the Cd(II) removal rate showed a smooth plateau trend when further adsorbents were added. Apparently, the removal rate and adsorption capacity of SWM were higher than OW. The high removal efficiency of Cd(II) from aqueous solution by SWM and its remarkable adsorption performance was due to the presence of functional groups on SWM. When the dosage of OW was 2 g/L, the Cd(II) removal rate reached the highest at 44.40%. When the dosage of SWM was 15 g/L, the Cd(II) removal rate reached the highest at 99.86%. When the adsorbent dosage was lower, the adsorption capacity was higher. This was because when the initial concentration of the solution is constant, the less the adsorbent, the more the adsorbate[Cd(II)] which can be combined with adsorbent mass per unit mass, and the larger the adsorption capacity. Fewer adsorbents provided less active sites, therefore the removal rates were lower. Hence, as the dosage increased, the adsorption amount decreased and the removal rate increased. The optimum adsorbent dosage of SWM was determined to be 15 g/L for further study.

3.2.3. Effect of contact time and kinetic modeling

Fig. 8 shows the Cd(II) removal of OW and SWM under different contact time, in order to explore the effect of

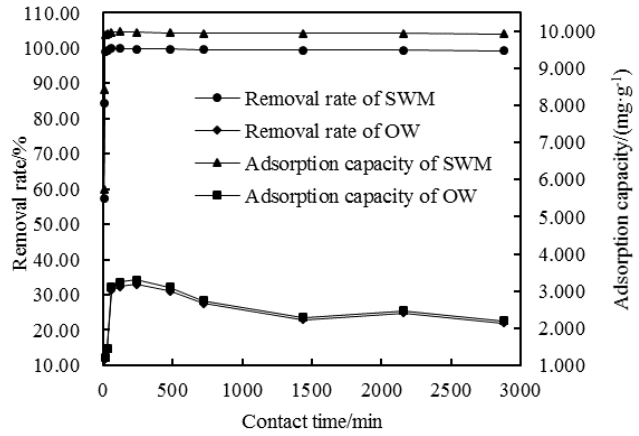

Fig. 8. Effect of contact time on Cd(II) adsorption.

contact time on adsorption and the adsorption kinetics of Cd(II) removal of SWM. As seen from the results in figure, the Cd(II) removal rate of SWM had reached 99.08% in 15 min, while the Cd(II) removal rate of OW only reached 11.92% under the same condition. And the removal rate of SWM was always higher than OW, indicating that the adsorbent modified by this modification method had an excellent adsorption effect on Cd(II).

The experimental data of SWM were analyzed by pseudo-first-order kinetic model, pseudo-second-order kinetic model and intraparticle diffusion model. The relevant parameters are given in Table 2. It can be seen from the table that the Cd(II) adsorption of SWM did not conform to the pseudo-first-order kinetic model (R^2 = 0.0174), and some scholars had obtained similar results [39]. However, further analysis showed that the pseudo-first-order kinetic equation was only applicable to the initial stage of the adsorption process, rather than the entire contact time range. The pseudo-second-order model perfectly described the Cd(II) adsorption of SWM (R^2 = 1). According to the assumption of the pseudo-second-order kinetic model, the adsorption process of SWM was mainly limited by chemical adsorption, that is, the adsorption process was completed by electrons exchange and sharing between adsorbate [40]. Similar results have

Table 2
Kinetic parameters of Cd(II) adsorption of SWM

Pseudo-first-order kinetics			Pseudo-second-order kinetics		
q_e (mg g^{-1})	K_1 (min^{-1})	R^2	Q_e (mg g^{-1})	K_2 (g/mg min)	R^2
0.09	0.0002	0.0174	9.93	1.5364	1.000

Intraparticle diffusion model								
$K_{id,1}$ (mg g^{-1} min$^{-0.5}$)	$C_{id,1}$ (mg g^{-1})	R^2	$K_{id,2}$ (mg g^{-1} min$^{-0.5}$)	$C_{id,2}$ (mg g^{-1})	R^2	$K_{id,3}$ (mg g^{-1} min$^{-0.5}$)	$C_{id,3}$ (mg g^{-1})	R^2
2.5926	0.0122	0.9986	0.0195	9.8305	0.9966	–0.0013	9.9946	0.9484

been reported in other related studies [35,41]. In addition, the q_e value calculated by the pseudo-second-order equation was agreed well with the experimental q_e value. In order to further determine the diffusion mechanism of the Cd(II) adsorption process, the intraparticle diffusion equation was studied. It can be seen from Fig. 9 that the linear graph of the intraparticle diffusion model of Cd(II) was multi-segmented, it is divided into three sections, corresponding to the three stages of the whole adsorption process, namely rapid adsorption, slow adsorption and equilibrium adsorption. From Table 2, $K_{id,1}$ was the maximum value among the values of the diffusion rate constants, indicating that the rapid adsorption plays a major role in the whole adsorption process. When the active sites on the surface of SWM were completely occupied, Cd(II) gradually shifted to internal diffusion, and bound to the internal active sites. At this time, the adsorption rate decreased as the mass transfer resistance became larger, that is, the slow adsorption process. Then the concentration of Cd(II) and the active sites of SWM gradually decreased, the adsorption rate eventually tended to zero and reached the adsorption equilibrium stage. So the Cd(II) adsorption of SWM was controlled by surface adsorption and intraparticle diffusion. Besides, the $C_{id,2}$ and $C_{id,3}$ values are large, indicating that surface adsorption was dominant in the entire adsorption process.

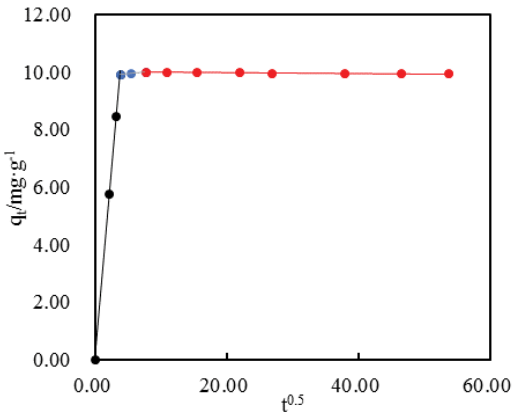

Fig. 9. Curve of intraparticle diffusion model.

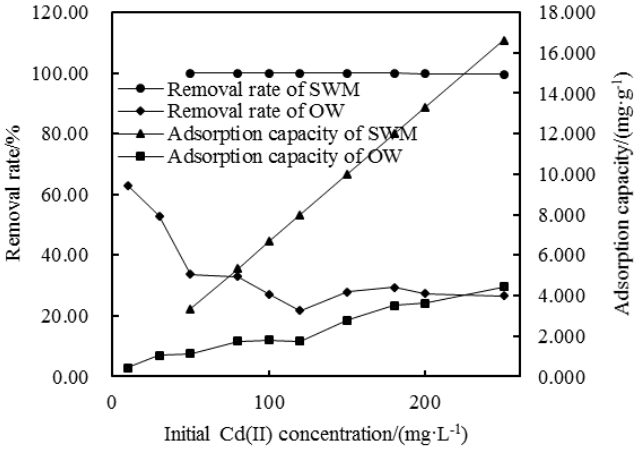

Fig. 10. Effect of initial Cd(II) concentration on Cd(II) adsorption.

3.2.4. *Effect of initial Cd(II) concentration and isotherm modeling*

Fig. 10 shows the Cd(II) removal of OW and SWM in solution with different initial Cd(II) concentration, in order to explore the effect of initial Cd(II) concentration on adsorption and the adsorption isotherm of Cd(II) removal of SWM. As shown in Fig. 10, the Cd(II) removal rate of SWM was maintained above 99% regardless of the initial concentration of Cd(II), the adsorption performance was great. However, OW only showed a high Cd(II) removal capacity under low concentration conditions, and the maximum removal rate took place at 10 mg/L, which reached 62.90%, and then showed a downward trend. This can be explained by the adsorption dependence on the availability of the binding sites on adsorbent surface [39].

The experimental data of SWM were analyzed by Langmuir isotherm, Freundlich isotherm and Temkin isotherm. The relevant parameters are given in Table 3. It can be seen from the table that the Langmuir isotherm fitted best (R^2 = 0.9921). The Langmuir isotherm model is based on the assumption that all adsorption sites of the adsorbent have the same energy [32], the maximum mono-layer adsorption will happen when the molecules absorbed on the surface of the adsorbent form a saturated layer [42,43]. It is indicated that the Cd(II) adsorption of SWM was mainly mono-layer adsorption, and the interaction between the adsorbed Cd(II) after the adsorption reached saturation was negligible [43]. In addition, a dimensionless equilibrium parameter R_L is often used to determine the feasibility of the adsorption process. The adsorption process confirms to be unfavorable (R_L > 1), linear (R_L = 1), favorable (0 < R_L < 1) or irreversible

(R_L = 0) [44]. All of the calculated R_L were between 0 and 1, so the Cd(II) adsorption of SWM was favorable. The Freundlich isotherm describes non-ideal multilayer adsorption that occurs on non-uniform surfaces. It can be seen from Table 3 that the calculated 1/n value was between 0 and 1, indicating that the Cd(II) adsorption of SWM was favorable. However, the adsorption showed a worse fit with the Freundlich isotherm than any other isotherm studied in this paper (R^2 = 0.8285). The Temkin isotherm is based on the assumption that the heat of adsorption of all molecules in layer decreases linearly with coverage of adsorbent surface because of the interactions between adsorbate and adsorbent, and the adsorption energy is not uniform [45]. The Temkin isotherm fitted better than the Freundlich isotherm (R^2 = 0.9218). The larger the a_T value is, the larger the negative value of the Gibbs free energy of the adsorption is, and makes it more available for the adsorption process. Therefore, the a_T value given in table demonstrated that the Cd(II) adsorption by SWM was easy to carry out.

The adsorption capacity of adsorbents reported in the literature on Cd(II) was compared with the SWM obtained in this study (Table 4). The high capacity of SWM compare well with other adsorbents.

3.2.5. Effect of adsorption temperature and thermodynamic study

Fig. 11 shows the Cd(II) removal of OW and SWM in solution at different temperature, in order to explore the effect of temperature on adsorption and the adsorption thermodynamic of Cd(II) removal of SWM. As shown in Fig. 11, although the Cd(II) removal rate of SWM maintained a high level, it still showed a down trend with the increase of temperature. And the Cd(II) removal rate of OW had the same trend, but it was always far less than the Cd(II) removal rate of SWM.

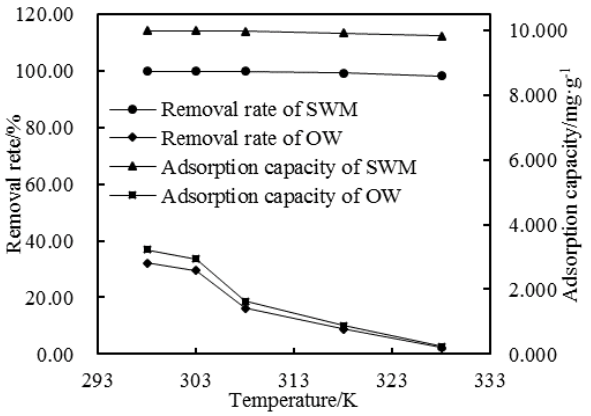

Fig. 11. Effect of temperature on Cd(II) adsorption.

The corresponding thermodynamic parameters of the Cd(II) adsorption on SWM were calculated and are listed in Table 5. It can be seen from the table that ΔH was a negative value, indicating that the Cd(II) adsorption process of SWM was an exothermic process, and the increase in temperature was not conducive to the adsorption, for example. ΔS was also a negative value, denoting that the chaos of the solid–liquid interface during adsorption was reduced. Moreover, ΔG gradually increased as the temperature increased, demonstrating that the degree of spontaneousness of the adsorption process was inversely proportional to temperature. And ΔG was a negative value, indicating that the Cd(II) adsorption of SWM was feasible and spontaneous.

3.3. Adsorption mechanism

The adsorption mechanisms of SWM were explored according to the results of SEM, BET, FT-IR, XPS and

Table 3
Isotherm parameters of Cd(II) adsorption of SWM

Langmuir isotherm			Freundlich isotherm			Temkin isotherm		
q_m/(mg g^{-1})	K_L/(L g^{-1})	R^2	K_F/(μg g^{-1})	n	R^2	a_T/(L mg^{-1})	b_T/(kJ mol^{-1})	R^2
17.79	11.2400	0.9921	19.3776	2.7020	0.8285	739.09	2.54	0.9218

Table 4
Comparison of Cd(II) adsorption capacity on SWM vs. other adsorbents

Materials	pH	Adsorption capacity/(mg g^{-1})	References
Oak wood char (fast pyrolysis 400°C)	5	0.4	[46]
Oak bark char (fast pyrolysis 450°C)	5	5.4	
Pine bark char (fast pyrolysis 400°C)	5	0.3	
Activated carbon, F-400	5	8.0	
Calcium-based magnetic biochar	6	10.07	[47]
Bacteria montmorillonite	5	8.23	[48]
Chitosan-pyromellitic dianhydride modified biochar	5	30.12	[49]
$KFeP_2O_7$ implanted on silica gel beads	6.5	5.076	[50]
SWM	7.0	17.79	This study

Table 5
Thermodynamic parameters of Cd(II) adsorption of SWM

Temperature/K	ΔG/kJ mol^{-1}	ΔH/kJ mol^{-1}	ΔS/kJ mol^{-1}
298	–166.03		
303	–145.96		
308	–125.92	–1,360.48	–4.01
318	–85.84		
328	–45.75		

adsorption experiments. It can be concluded that Cd(II) was mainly absorbed through complexation and ion exchange. The thiol group can react with heavy metal ions to form a complex, it can be described as follows:

$$2R–SH + Cd^{2+} \rightarrow R–S–Cd–S–R + 2H^{+} \quad (16)$$

The ion exchange can be described as follows:

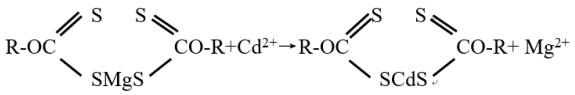

(17)

where *R* is organic group present for walnut shell.

4. Conclusion

A sulfur-functionalized walnut shell biochar was prepared through xanthogenization and modification for removing Cd(II) from aqueous solution. The characterization results of SWM concluded that the modification was beneficial to the Cd(II) adsorption, and the adsorption performance of SWM was better. The experimental results suggested that the optimum pH for Cd(II) adsorption was 7.0. The adsorption process of SWM was best fitted to the Langmuir adsorption isotherm model, indicating that the adsorption was mainly mono-layer adsorption and was favorable. The pseudo-second-order model and the intraparticle diffusion equation were more suitable for the adsorption process of SWM, and the adsorption equilibrium had been reached in a short time. The thermodynamic study indicated that the adsorption process of SWM was essentially feasible, spontaneous and exothermic. The Cd(II) adsorption on SWM was the result of a combination of complexation and ion exchange, moreover, –SH was the important functional group participated in the adsorption. Therefore, it is recommended to use xanthate-modified walnut shell as a cost-effective biosorbent, which has broad application prospects in the treatment of cadmium-contaminated water. This work provided a reliable basis for further application of walnut shell in actual contaminated water treatment.

Acknowledgment

This work was supported by the National Natural Science Foundation (51768018) of China.

References

[1] L.I. Xiaomin, Y. Tang, Z. Xuan, Y. Liu, L. Fang, Study on the preparation of orange peel cellulose adsorbents and biosorption of Cd^{2+} from aqueous solution, Sep. Purif. Technol., 55 (2007) 69–75.
[2] J.E. Lim, M. Ahmad, A.R.A. Usman, S.S. Lee, Effects of natural and calcined poultry waste on Cd, Pb and As mobility; in contaminated soil, Environ. Earth Sci., 69 (2013) 11–20.
[3] M. Shahid, S. Khalid, G. Abbas, N. Shahid, M. Nadeem, M. Sabir, M. Aslam, C. Dumat, Heavy Metal Stress and Crop Productivity, Cro. Prod. Glo. Environ. Iss., Springer International Publishing, 2015, pp. 1–25.
[4] N.K. Niazi, B. Singh, B. Minasny, Mid-infrared spectroscopy and partial least-squares regression to estimate soil arsenic at a highly variable arsenic-contaminated site, Int. J. Environ. Sci. Technol., 12 (2015) 1965–1974.
[5] H.P. Singh, P. Mahajan, S. kaur, D.R. Batish, Chromium toxicity and tolerance in plants, J. Environ. Biol., 11 (2013) 229–254.
[6] J. Liu, S. Yuan, H. Du, X. Jiang, Adsorption of Cd(II) from Aqueous Solution by Magnetic Graphene, Adv. Mater., 881–883 (2014) 1011–1014.
[7] T. Kawamoto, Selective removal of cesium ions from wastewater using copper hexacyanoferrate nanofilms in an electrochemical system, Electrochim. Acta, 87 (2013) 119–125.
[8] S.A. Kim, S. Kamala-Kannan, K.J. Lee, Y.J. Park, P.J. Shea, W.H. Lee, H.M. Kim, B.T. Oh, Removal of Pb(II) from aqueous solution by a zeolite–nanoscale zero-valent iron composite, Chem. Eng. J., 217 (2013) 54–60.
[9] M. Yusuf, F.M. Elfghi, S.A. Zaidi, Applications of graphene and its derivatives as an adsorbent for heavy metal and dye removal: a systematic and comprehensive overview, RSC Adv., 5 (2015) 50392–50420.
[10] G. Liu, Z. Wen, R. Luo, Synthesis, characterization of amino-modified walnut shell and adsorption for Pb(II) ions from aqueous solution, Polym Bull., 76 (2019) 1099–1114.
[11] K. Paria, S.M. Mandal, S.K. Chakroborty, Simultaneous removal of Cd(II) and Pb(II) using a fungal isolate, *Aspergillus penicillioides* (F12) from Subarnarekha Estuary, Int. J. Environ. Res., 12 (2018) 77–86.
[12] M.X. Tan, N.S. Yin, J.Y. Ying, Y. Zhang, A mesoporous polymelamine-formaldehyde polymer as a solid sorbent for toxic metal removal, Energy Environ. Sci., 6 (2013) 3254–3259.
[13] T.S. Natarajan, M. Thomas, K. Natarajan, H.C. Baja, Study on UV-LED/TiO_2 process for degradation of Rhodamine B dye, Chem. Eng. J., 169 (2011) 126–134.
[14] M. Feizi, M. Jalali, Removal of heavy metals from aqueous solutions using sunflower, potato, canola and walnut shell residues, J. Taiwan Inst. Chem. Eng., 54 (2015) 125–136.
[15] K. Osvaldo, L.V.A. Gurgel, J.C.P. Melo, De, B. Vagner Roberto, T.M.S. Melo, G. Laurent Frédéric, Adsorption of heavy metal ion from aqueous single metal solution by chemically modified sugarcane bagasse, Bioresour. Technol., 98 (2007) 1291–1297.
[16] G.N. Paranavithana, K. Kawamoto, Y. Inoue, T. Saito, M. Vithanage, C.S. Kalpage, G.B.B. Herath, Adsorption of Cd^{2+} and Pb^{2+} onto coconut shell biochar and biochar-mixed soil, Environ. Earth Sci., 75 (2016) 484.
[17] S. Guiza, Biosorption of heavy metal from aqueous solution using cellulosic waste orange peel, Ecol. Eng., 99 (2017) 134–140.
[18] A.C. Lua, T. Yang, Effect of activation temperature on the textural and chemical properties of potassium hydroxide activated carbon prepared from pistachio-nut shell, J. Colloid Interface Sci., 274 (2004) 594–601.
[19] F. Yang, Y. He, S. Sun, C. Yue, Z. Fei, Z. Lei, Walnut shell supported nanoscale Fe 0 for the removal of Cu(II) and Ni(II) ions from water, J. Appl. Polym. Sci., 133 (2016).
[20] M.K. Dahri, M.R.R. Kooh, L.B. Lim, Water remediation using low cost adsorbent walnut shell for removal of malachite green: equilibrium, kinetics, thermodynamic and regeneration studies, J, Environ, Chem, Eng,, 2 (2014) 1434–1444.
[21] D. Ding, Y. Zhao, S. Yang, W. Shi, Z. Zhang, Z. Lei, Y. Yang, Adsorption of cesium from aqueous solution using agricultural residue – walnut shell: equilibrium, kinetic and thermodynamic modeling studies, Water Res., 47 (2013) 2563–2571.
[22] R. Xie, H. Wang, Y. Chen, W. Jiang, Walnut shell-based activated carbon with excellent copper (II) adsorption and lower

chromium (VI) removal prepared by acid–base modification, Environ. Prog. Sustain., 32 (2013) 688–696.
[23] S.J. Segovia-Sandoval, R. Ocampo-Pérez, M.S. Berber-Mendoza, R. Leyva-Ramos, A. Jacobo-Azuara, N.A. Medellín-Castillo, Walnut shell treated with citric acid and its application as biosorbent in the removal of Zn (II), J. Water Proc. Eng., 25 (2018) 45–53.
[24] M. Zhu, J. Yao, L. Dong, J. Sun, Adsorption of naphthalene from aqueous solution onto fatty acid modified walnut shells, Chemosphere, 144 (2016) 1639–1645.
[25] K. Chomiak, S. Gryglewicz, K. Kierzek, J. Machnikowski, Optimizing the properties of granular walnut-shell based KOH activated carbons for carbon dioxide adsorption, J. CO_2 Util., 21 (2017) 436–443.
[26] R.G. Pearson, Hard and Soft Acids and Bases, Sur. Prog. Chem., 5 (1969) 1–52.
[27] X.g. Lu, Y.t. Guo, Removal of Pb (II) from aqueous solution by sulfur-functionalized walnut shell, Environ. Sci. Pollut. Res., (2019) 1–12.
[28] T. Zhou, F. Xia, Y. Deng, Y. Zhao, Removal of Pb(II) from aqueous solutions using waste textiles/poly(acrylic acid) composite synthesized by radical polymerization technique, J. Environ. Sci.-China, 67 (2018) 371–380.
[29] S.Srivastava, S.B. Agrawal, M.K. Mondal, Synthesis, characterization and application of *Lagerstroemia speciosa* embedded magnetic nanoparticle for Cr(VI)adsorption from aqueous solution, J. Environ. Sci., 55 (2017) 283–293.
[30] X. Zhao, X. Zeng, Y. Qin, X. Li, T. Zhu, X. Tang, An experimental and theoretical study of the adsorption removal of toluene and chlorobenzene on coconut shell derived carbon, Chemosphere, 206 (2018) 285.
[31] R.G.P. Viera, G.R. Filho, R.M.N.D. Assunção, C.D.S. Meireles, J.G. Vieira, G.S.D. Oliveira, Synthesis and characterization of methylcellulose from sugar cane bagasse cellulose, Carbohydr. Polym., 67 (2007) 182–189.
[32] Z. Sheng, Y. Shen, H. Dai, S. Pan, B. Ai, L. Zheng, X. Zheng, Z. Xu, Physicochemical characterization of raw and modified banana pseudostem fibers and their adsorption capacities for heavy metal Pb^{2+} and Cd^{2+} in water, Polym. Compos., 39 (2018) 1869–1877.
[33] Z. Wenbing, G. Xuan, Z. Duanwei, L. Alan, D. Li, H. Yumei, Z. Jianwei, Metal adsorption by quasi cellulose xanthogenates derived from aquatic and terrestrial plant materials, Bioresour. Technol., 102 (2011) 3629–3631.
[34] X.F. Sun, F. Xu, R.C. Sun, P. Fowler, M.S. Baird, Characteristics of degraded cellulose obtained from steam-exploded wheat straw, Carbohydr. Res., 60 (2005) 15–26.
[35] Y. Chen, J. Wang, The characteristics and mechanism of Co(II) removal from aqueous solution by a novel xanthate-modified magnetic chitosan, Nucl. Eng. Des., 242 (2012) 452–457.
[36] X. Liang, X.U. Yingming, G. Sun, W. Lin, S. Yang, X.U. Qin, Preparation, characterization of thiol-functionalized silica and application for sorption of Pb^{2+} and Cd^{2+}, Colloid Surf., A, 349 (2009) 61–68.
[37] J. Qu, X. Meng, X. Jiang, H. You, P. Wang, X. Ye, Enhanced removal of Cd(II) from water using sulfur-functionalized rice husk: characterization, adsorptive performance and mechanism exploration, J. Cleaner Prod., 183 (2018) 880–886.
[38] Y. Zhu, J. Hu, J. Wang, Removal of Co^{2+} from radioactive wastewater by polyvinyl alcohol (PVA)/chitosan magnetic composite, Prog. Nucl. Energy, 71 (2014) 172–178.
[39] A. Sari, M. Tuzen, Cd(II) adsorption from aqueous solution by raw and modified kaolinite, Appl. Clay Sci., 88–89 (2014) 63–72.
[40] E. Igberase, P. Osifo, Equilibrium, kinetic, thermodynamic and desorption studies of cadmium and lead by polyaniline grafted cross-linked chitosan beads from aqueous solution, J. Ind. Eng. Chem., 26 (2015) 340–347.
[41] H. Ren, Z. Gao, D. Wu, J. Jiang, Y. Sun, C. Luo, Efficient Pb(II) removal using sodium alginate–carboxymethyl cellulose gel beads: preparation, characterization, and adsorption mechanism, Carbohydr, Polym., 137 (2016) 402–409.
[42] Z. Wang, J.P. Barford, W.H. Chi, G. Mckay, Kinetic and equilibrium studies of hydrophilic and hydrophobic rice husk cellulosic fibers used as oil spill sorbents, Chem. Eng. J., 281 (2015) 961–969.
[43] Z.A. Sutirman, M.M. Sanagi, K.J.A. Karim, A.W.I. Wan, B.H. Jume, Equilibrium, kinetic and mechanism studies of Cu(II) and Cd(II) ions adsorption by modified chitosan beads, Int. J. Biol. Macromol., 116 (2018) 255–263.
[44] S. He, Y. Li, L. Weng, J. Wang, J. He, Y. Liu, K. Zhang, Q. Wu, Y. Zhang, Z. Zhang, Competitive adsorption of Cd^{2+}, Pb^{2+} and Ni $^{2+}$ onto Fe^{3+} -modified argillaceous limestone: influence of pH, ionic strength and natural organic matters, Sci. Total Environ., 637–638 (2018) 69–78.
[45] A.S. Cukrowski, Equilibrium uptake, isotherm and kinetic studies of Cd(II) adsorption onto iron oxide activated red mud from aqueous solution, J. Mol. Liq., 202 (2015) 165–175.
[46] D. Mohan, C.U.P. Jr., M. Bricka, Sorption of arsenic, cadmium, and lead by chars produced from fast pyrolysis of wood and bark during bio-oil production, J. Colloid Interface Sci., 310 (2007) 57–73.
[47] J. Wu, D. Huang, X. Liu, J. Meng, C. Tang, J. Xu, Remediation of As(III) and Cd(II) co-contamination and its mechanism in aqueous systems by a novel calcium-based magnetic biochar, J. Hazard. Mater., 348 (2018) 10–19.
[48] P. Cai, H. Du, X. Rong, X. Feng, W. Chen, Q. Huang, Competitive adsorption of Pb and Cd on bacteria-montmorillonite composite, Environ. Pollut., 218 (2016) 168–175.
[49] J. Deng, Y. Liu, S. Liu, G. Zeng, X. Tan, B. Huang, X. Tang, S. Wang, Q. Hua, Z. Yan, Competitive adsorption of Pb(II), Cd(II) and Cu(II) onto chitosan-pyromellitic dianhydride modified biochar, J. Colloid Interface Sci., 506 (2017) 355–364.
[50] E. Ordoñez-Regil, F. Granados-Correa, E. Ordoñez-Regil, M.G. Almazán-Torres, Nanoparticles of $KFeP_2O_7$ implanted on silica gel beads for Cd2+ ion adsorption, Environ. Technol., 36 (2015) 188–197.